Development and Testing of a Vine Robot for Urban Search and Rescue in Confined Rubble Environments

Zheyu Zhou [1], Yaqing Wang [1], Elliot W. Hawkes [2], Chen Li [1]

***Abstract*— The request for fast response and safe operation after natural and man-made disasters in urban environments has spurred the development of robotic systems designed to assist in search and rescue operations within complex rubble sites. Traditional Unmanned Aerial Vehicles (UAVs) and Unmanned Ground Vehicles (UGVs) face significant limitations in such confined and obstructed environments. This paper introduces a novel vine robot designed to navigate dense rubble, drawing inspiration from natural growth mechanisms found in plants. Unlike conventional robots, vine robots are soft robots that can grow by everting their material, allowing them to navigate through narrow spaces and obstacles. The prototype presented in this study incorporates pneumatic muscles for steering and oscillation, an equation-based robot length control plus feedback pressure regulating system for extending and retracting the robot body. We conducted a series of controlled experiments in an artificial rubble testbed to assess the vine robot's performance under varying environmental conditions and robot parameters, including volume ratio, environmental weight, oscillation, and steering. The results show that the vine robot can achieve significant penetration depths in cluttered environments with mixed obstacle sizes and weights, and can maintain repeated trajectories, demonstrating potential for mapping and navigating complex underground paths. Our findings highlight the vine robot's suitability for urban search and rescue missions, with further research planned to enhance its robustness and deployability in real-world scenarios.**

Keywords—vine robot, bio-inspired robotics, rescue robots, urban search and rescue.

I. Introduction

In recent years, the application of robots in specialized tasks has become increasingly common, particularly in roles where they extend the capabilities of emergency professionals in disaster response [1]. A significant area of focus is the development of search and rescue robots designed for deployment in urban rubble sites following natural or man-made disasters [2]. Various types of robots have been engineered to address specific challenges in these environments. For instance, Unmanned Aerial Vehicles (UAVs) are utilized for aerial reconnaissance of disaster sites, providing critical overviews of the affected areas [3, 4]. Unmanned Ground Vehicles (UGVs) are deployed to navigate spaces that are inaccessible to conventional vehicles, including structures that pose safety risks for human entry [4, 5, 6].

While ground robots hold immense potential in urban search and rescue missions, their mobility is often compromised in complex environments characterized by unpredictable obstacles of varying sizes, shapes, and surfaces. Researchers have developed rover-like and legged robots capable of traversing uneven terrain [4, 7]. However, the intricate nature of urban disaster zones often limits the effectiveness of these robots, particularly in navigating through rubble. Other robotic systems, such as crawlers and snake-like robots, have been designed to access confined spaces like tunnels and caves, yet they struggle to maneuver within densely compacted debris [8, 9].

The search and rescue in urban disaster sites is a race against time. According to the report from [1, 10, 11], the gold-saving time for urban rubble search and rescue is 48 hours, and among all the survivors rescued from the rubble, only 20% of survivors were found deep under the rubble. Most survivors could be found close to the top surface of the rubble within the gold 48 hours saving time as the first responders would normally rely on manual methods until the later clearance on the roads to deliver more large tools and machinery on site. Therefore, it is necessary to reach deep down into the rubble quickly after the disaster happened and complete the search and medical support for the people trapped under the rubble, and as it was not feasible to let responders enter the internal of the rubble site without proper tools and protections, a robot would be perfect to perform the search and rescue task for the trapped people after the disaster happened.

Interestingly, the natural world offers inspiration for overcoming the challenge of reaching deep down and transporting goods in a complicated environment. The way vines or plant roots extend through the ground provides a potential model for robotic movement in confined and obstructed spaces [12, 13]. Recently, the development of vine robots has shown promise in addressing some of the limitations faced by traditional search and rescue robots. These robots have been used for various tasks, including serving as antenna holders [14], acting as jacks [15], and inspecting tunnels [16]. The versatility of vine robots is attributed to several unique features. As a type of soft robot, a vine robot grows by everting material from its tip while the external wall of its body remains stationary. This allows the robot to deform and squeeze through crevices smaller than its tip diameter [15]. Additionally, vine robots are equipped with pneumatic muscles that enable precise steering as they navigate through complex environments [17, 18, 19].

[1] Dept. of Mechanical Engineering, Johns Hopkins University. [2] Dept. of Mechanical Engineering, University of California, Santa Barbara.
Corresponding Author: chen.li@jhu.edu, https://li.me.jhu.edu

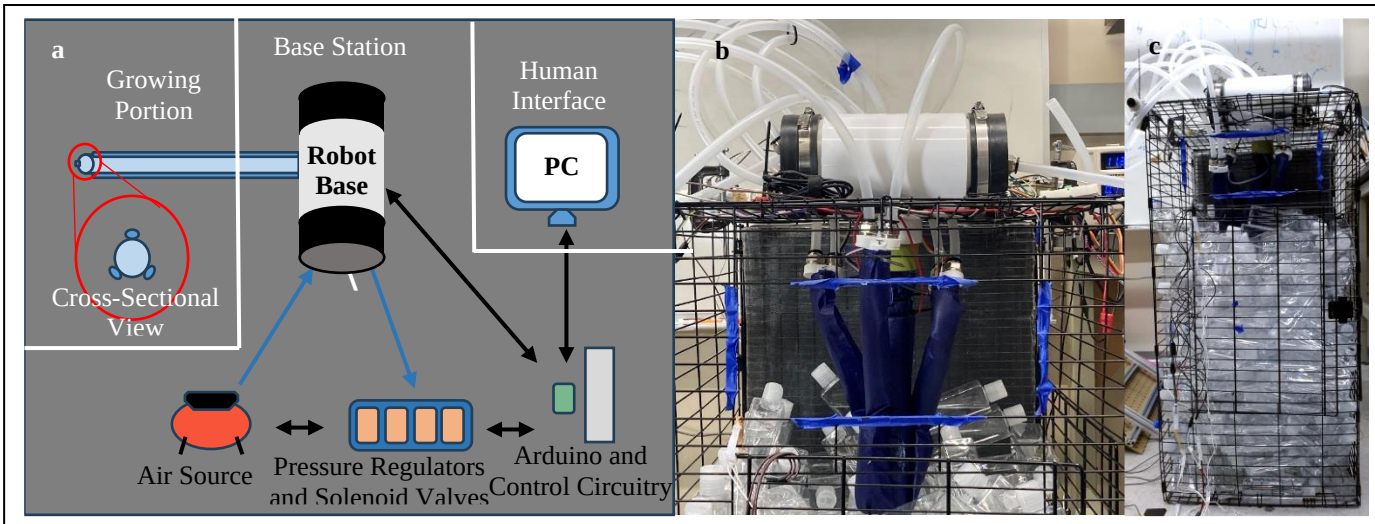

Fig. 1. Vine Robot Prototype. (a) Robot prototype built in the lab. (b) Robot prototype components. (c) Testbed combined robot system and artificial environment.

Given these capabilities, vine robots show significant potential for urban search and rescue operations, where constant interaction with diverse obstacles is required. Their high mobility, facilitated by a lightweight, rip-resistant fabric body, allows them to be easily transported in a backpack to the deployment site, enabling rapid response in disaster scenarios. Moreover, vine robots can be equipped with a variety of tools, such as tip-mounted cameras for internal inspection [16], tubes fixed inside the wall [20] for the delivery of medical supplies or food, and antennas to enhance communication signals at the disaster site [14]. These features make vine robots a compelling candidate for use in search and rescue missions within urban rubble environments.

II. Initial Development and Testing

A. *Initial Prototype Design*

The initial prototype of our vine robot was adapted from a previously established robotic system [21] to suit the specific conditions of our study. This prototype consists of three main components: the robot base station, the human interface, and the growing vine body (Fig. 1).

The robot base station integrates a pressure container, a motorized vine body spool, and all necessary electronics. The pressure container, constructed from PVC pipes, is sealed with Qwik Caps. The pressure is supplied from a building air source and monitored using an MPRLS 3965 (Adafruit) pressure sensor. The system also includes solenoid valves and an Arduino-Uno, which together enable feedback control on pressure. The motorized vine body spool is driven by an XM-430 (Dynamixel) motor, controlled by an OpenRB-150 (Dynamixel) controller, allowing for the growth and retraction of the vine robot. The angular readings from the motor are used to estimate the vine body's length, applying the Archimedean spiral equation, as shown in Eqn. 1. Once the estimated length reaches the maximum length of the vine robot, the robot will stop growing and start retracting the vine body. The parameters of the equation are defined as follows:

- r: Distance from the center of the spiral to its outermost edge.
- α: Total swept angle of the spiral, which captures the angular displacement over which the spiral extends.
- a: Measured separation distance between consecutive turns of the spiral.
- b: Spiral offset, equivalent to the radius of the spooling bar.
- L: The arc length of the spiral, calculated from these parameters, which corresponds to the length of the vine robot.

$$r = \alpha a + b$$
$$L = \int_b^r \sqrt{(\alpha(r))^2 + (\frac{d\alpha}{dr})^2}\, dr \quad (1)$$

$$L = \frac{1}{a}\left[\frac{(r-b)}{2}\sqrt{(r-b)^2+1} + \frac{1}{2} ln(r-b+\sqrt{(r-b)^2+1})\right]$$

The two divided subsystems, the pressure regulation system and the vine body length control system are programmed to communicate via customized protocols to ensure the safe and robust operation of the robot, allowing the robot to endure at least five hours of continuous operation for our experiments. These system statuses were presented through the Arduino IDE Serial Port display. The Serial Port showed container pressure, vine body length, and indicators of growth or retraction on the computer screen for human interface.

The growing soft vine body (Fig. 1b) was fabricated using double-wall silicon-coated rip-stop Nylon fabric (Rockywoods

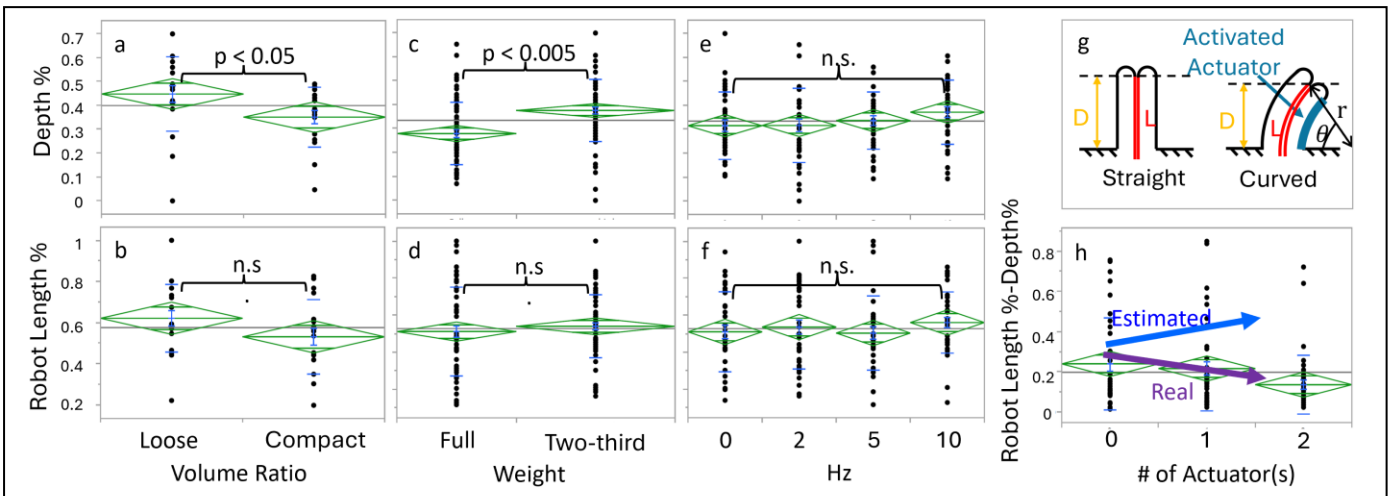

Fig. 2. Experiment Data Analysis. Data analysis using One-way ANOVA method to study the normalized ratio values of robot grown length and the reached depth over the longest possible length of the robot with different environmental or robot parameters. (a, b) Robot depth% and length% comparison under loose and compact environmental volume ratio settings. (c, d) Robot depth% within full-filled-bottle heavy environment and two-third-filled-bottle light environment. (e, f) Robot depth% and length% comparison with changing robot oscillations. (g) Demonstration of steered vine robot shape in the free space and the difference between robot length and reachable depth when robot is actuated to curve. (h) Comparing difference in robot length% and depth% with different number of activated steering actuators.

Fabrics) and room-temperature vulcanizing silicon adhesive (SilPoxy, Smooth-On). In this initial phase, the vine body was built to 430 mm to mitigate boundary effects caused by jamming the obstacles next to the boundary of the testbed. Along the vine body, three equally spaced fabric pneumatic artificial muscle (fPAM) actuators were incorporated to introduce oscillation, thereby enabling random tip-pointing directions. The fPAM was used due to their low hysteresis and high contraction ratio.

To evaluate the vine robot's performance in cluttered and heavy rubble environments, we constructed a testbed (Fig. 1c). The robot system is mounted on the top, while the bottom houses a rubble-mimicking environment. The testbed was built upon a 430 mm x 430 mm x 930 mm cage filled with plastic bottles of same sizes and weights, creating a semi-transparent and mono-dispersed artificial rubble environment. This setup allows the vine robot to interact with the rubble, while also enabling us to observe its trajectories and movements through front-view and side-view cameras that record all trials.

B. Experiment and Performance

In our initial experiments, we aimed to investigate how the environmental parameters and robot settings would influence the vine robot's performance. The performance is measured by the ratio of the length of robot growth to its maximum length and the ratio of the robot reached depth to the maximum length. The robot was programmed with pressure feedback control and body length feedforward control to achieve a semi-automatic systematic experiment that swept all the parameters and settings.

i. Volume Ratio

In the paper [22] studied robot locomotion in granular media, the granular media is a mono-dispersed environment with small filled-in particles relative to the robot intruder, we found that the robot locomotion performance is related to environment volume ratio. The volume ratio was defined as the ratio of the volume occupied by obstacles to the total volume. Thus, we hypothesized that the volume ratio would also affect vine robot's behavior while the robot is burrowing into the artificial rubble environment.

To adjust this ratio, we kept the overall volume constant while varying the number of bottles placed in the cage, implementing a few layers of rope nets with negligible volume and a grid size larger than the robot's diameter to reduce compactness without affecting the robot's trajectory. The obstacle-occupied volume was calculated by multiplying the number of bottles by the pre-measured volume of a single bottle. The total volume was determined by multiplying the cage's horizontal cross-sectional area by the occupied height.

To assess the impact of the volume ratio on the robot's performance, we compared the depth and length reached by the robot in both loose and compacted environments. The data (Fig. 2a, b) indicated that in a lower volume ratio environment, the robot penetrated deeper, although there was no significant difference in the overall length of the robot's growth.

ii. Environmental Weight

Based on the Resistive Force Theory [22] and the vine robot extension model [23], we hypothesized that the environment weight would be related to the vine robot burrowing performance as the vine robot tip-extension force would be balanced by the resistance force from the environment.

To alter the overall environmental weight, we adjusted the water level in each bottle while maintaining the same number of bottles used in each weight setting. The overall environmental weight was calculated by multiplying the number of bottles by their average weight.

We compared the robot's performance with bottles fully filled and two-thirds filled. The results showed that the robot achieved greater depth in the lighter, two-thirds-filled environment, yet the growth length remained unchanged across both settings (Fig. 2c, d).

iii. Robot Oscillation

The previous paper using oscillation additional energy to overcome the kinematic-potential energy threshold [] to reach a global minimum inspired us to see if we could introduce some oscillation to the robot and if it would be effective in helping the robot's performance.

We randomly turned on and off each fPAM actuator to use their inflation and deflation for creating the oscillation. The oscillation frequency was set from 2 Hz, 5 Hz, and 10 Hz to see the oscillation impact on robot performance.

The data (Fig. 2e, f) shows that there was no significance among all frequencies we used, thus introducing the oscillation might not improve the robot's performance after all.

iv. Actuated Steering

Lastly, we were interested in how we could maneuver the robot when the robot was constantly interacting with the rubble environment. So, we tried to activate the fPAM actuator(s) to curve the vine robot to see the influence on robot performance.

In free space, activating the fPAM causes the actuator to expand its girth and contract its length, curving the vine body. However, in the cluttered obstacle environment, the expected steering effect was not observed. Instead, the robot exhibited a reduced difference between depth and length as the number of activated actuators increased, which was initially supposed be an increased number as more actuators could curve the robot stronger (Fig. 2g). In fact, activating the steering actuators in a cluttered environment did not assist the robot in steering but rather helped it maintain a straighter down trajectory (Fig. 2h).

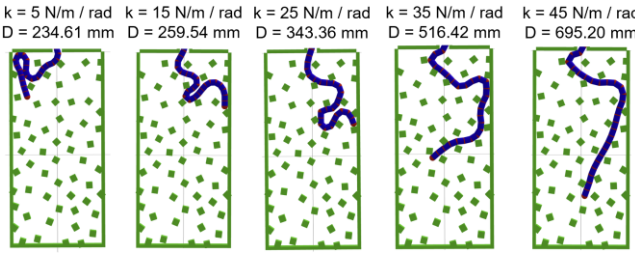

Fig. 3. Vine robot simulation with varying stiffness in the same cluttered environment.

C. Reveal Abnormal Performance

In a previous study which characterized the effect of actuation pressure lengthening [], it suggested that the stiffness of a soft robot body is influenced by the air pressure within it. Consequently, our pneumatic fPAM actuators were also stiffened during their actions, functioning like reinforcement ribs along the vine robot body, thereby increasing its overall stiffness. We hypothesize that this increased stiffness is responsible for the robot's tendency to move straight down rather than following a curved path.

To test this hypothesis, we adapted a Lagrange Multiplier-based dynamic model from previous research [] to simulate vine robot performance. We modified the open-source simulation code [] to create a 2D 430mm x 930mm cluttered environment with randomly spaced squares and varied the stiffness to observe its effects.

In the simulation, the robot's maximum length was set to 1000 mm, and stiffness was varied from 5 N/mm/rad to 45 N/mm/rad—an empirical threshold that could be achieved by pressurizing the vine robot to near-burst levels. The simulation results (Fig. 3) demonstrated that increased stiffness allowed the robot to penetrate deeper with fewer deflections in shallower regions, supporting our hypothesis.

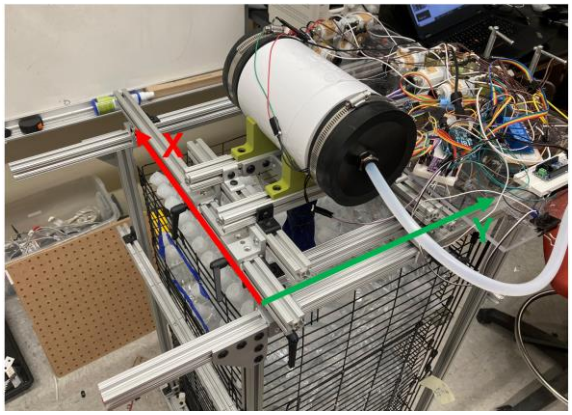

Fig. 4. X-Y gantry for different starting position.

III. Refined Robot and Experiment Testbed Design

A. Refined Prototype and Testbed Design

Following our initial experiments, we made improvements to our test environment to better simulate real urban rubble conditions. Based on the research [] that analyzed the composition of urban rubble disasters, they categorized the rubble into three types: small obstacles such as bricks, tiles, and natural stones, which constitute approximately 45% of the total volume; larger obstacles like concrete and debris, which account for another 45%; and thin metal gutters and sheathes, which make up the remaining 10%. In our testbed, we followed the composition ratio and represented these materials using bundled bottles and acrylic sheets. Small obstacles were simulated with bundles of less than four bottles, larger obstacles with bundles of four to ten bottles, and the thin metal elements were represented by acrylic sheets.

To enable precise control of the robot's starting position, we built an X-Y axis gantry using 20 mm x 20 mm aluminum profiles and sliders (Fig. 4). This gantry allows the robot to begin burrowing at any position between 110 mm and 320 mm in the X direction and between 140 mm and 290 mm in the Y direction. To compensate for the additional height introduced by the X-Y gantry, we increased the total depth of the rubble environment

by 300 mm, ensuring that the robot would immediately engage with the rubble, consistent with the conditions of the initial experiments. Additionally, the vine robot's length was extended to account for the increased depth of the environment.

B. *Experiment and Performance*

We tested the robot's performance in the newly refined testbed, which more accurately represents an urban rubble environment, using the X-Y gantry for starting position control. The experiment was semi-automated, with the robot capable of repeated growth and retraction, requiring only manual adjustments of the gantry to change the starting position.

In comparing the vine robot's performance in a mono-dispersed environment (with uniform obstacles) to that in a poly-dispersed environment (with varied obstacle sizes), we observed notable differences. In the mono-dispersed environment, the uniform obstacles tended to surround the robot consistently, causing it to squeeze and deflect frequently. These obstacles also increased the likelihood of encountering surfaces perpendicular to the robot's growth direction, which could block further growth (Fig. 5a).

Conversely, in the poly-dispersed environment, where obstacles varied in size, the robot grew along long ramps formed by the larger obstacles until its tip was deflected, squeezed, or halted by another obstacle (Fig. 5b). We found that in the new poly-dispersed environment, the obstacles were interlocked and remained stationary during robot interaction, unlike the easily moved bottles in the mono-dispersed setting. This stability allowed the vine robot to grow longer and deeper, and the stationary nature of the environment facilitated repeated growth and retraction along similar trajectories, as illustrated by the robot contours in (Fig. 5b).

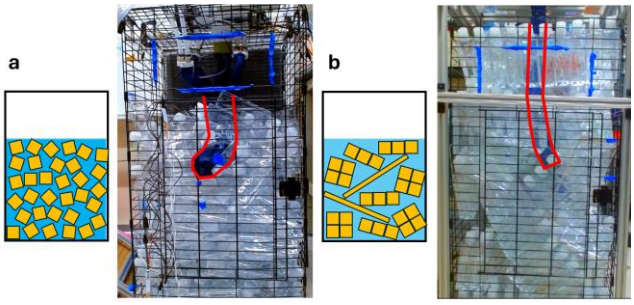

Fig. 5 Vine robot contour with obstacle environments. (a) Mono-dispersed environment. (b) Poly-dispersed environment.

C. *Potential Usage for Rubble Exploration*

The ability to achieve repeated trajectories in a fixed environment suggests that the vine robot could be used to map underground paths. Some researchers have developed shape sensors to measure the real-time shape of the vine robot [24]. However, these methods often require expensive sensors, such as Fiber Bragg Grating (FBG) sensors or distributed bending sensors. For our experiments, we opted for a more cost-effective solution using DLTdv8 to optically track the robot's trajectory.

First, we used DLTdv8 to calibrate the homography matrix by identifying crossing points on the cage and measuring the distances between them. We then tracked the robot's movement frame by frame, recording precise pixel readings. These readings were subsequently converted back to X-Z or Y-Z planes, depending on the camera view. Finally, we applied a nonlinear least squares method to minimize errors in the 3D reconstruction of the robot's path.

The resulting plot (Fig. 6) shows that when the robot starts in the range of $x = 150 \pm 50\,mm$ and $y = 150 \pm 20mm$, it consistently follows a path down to a shared crossing point. This result suggests that deploying one or more vine robots equipped with shape-sensing technology at an urban disaster site could help map the underground path structure, thereby facilitating more effective rescue planning.

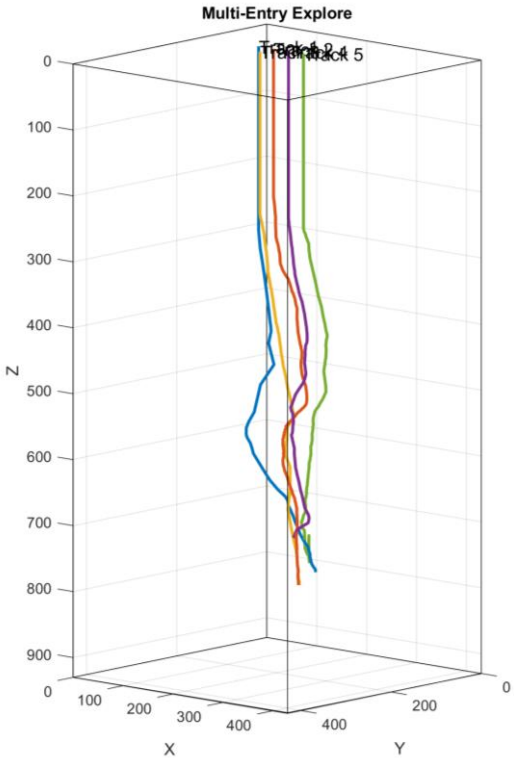

Fig. 6 Multi-Entry point exploration.

IV. Summery and Future Works

Many existing robots designed for disaster response are primarily intended for movement in free spaces of caves, tunnels, or paths [4]—[9], and even other vine robots have typically operated in less confined environments [15, 16]. In contrast, we have developed a vine robot capable of burrowing through densely packed heavy rubble, and we have designed a corresponding testbed to evaluate its performance in such challenging conditions. Our approach includes using relatively

low-cost and straightforward methods to simulate the vine robot's operations in complex and confined rubble spaces.

Through systematic testing, we explored how various factors influence the robot's performance. Our research involved iterative development phases, during which we investigated the potential applications of vine robots in disaster scenarios. We discovered that the vine robot could effectively navigate a poly-dispersed environment that simulates urban rubble, and we also explored future use cases, such as repeated material transport and multi-point entry for underground terrain exploration.

Our work opens up several avenues for further research. On the software side, we could enhance our simulator by expanding it to a 3D environment and designing a user interface that allows for better customization of obstacle physical properties. Additionally, updating the model of vine robot to incorporate more realistic non-linear mechanical characteristics to improve its accuracy.

In terms of hardware, we plan to equip the vine robot with more advanced shape sensors to provide precise real-time feedback on its shape. We could also improve the gantry system to allow the robot to enter the environment from different starting angles. Furthermore, upgrading the robot's fabric to more pressure-resistant and durable materials would enable it to operate in more challenging conditions.

Finally, expanding our research to outdoor environments and collaborating with professionals from search and rescue teams will be crucial steps toward developing a robot that can be deployed in real-world disaster scenarios. Additionally, we also aim to refine our testbed by incorporating more realistic materials and sensor combinations to better observe and test the robot's performance. We are looking forward to expanding our testbed into a test site that can model different urban disaster scenarios, providing a versatile testing ground not only for vine robots but for a variety of robotic systems.

REFERENCES

[1] R. R. Murphy, "Search and rescue robotics," in *Springer Handbook of Robotics*, Springer, 2007, pp. 1151–1173.

[2] J. Casper, M. Micire, and R. Murphy, "Issues in intelligent robots for search and rescue," in *Proc. SPIE*, pp. 292–302, 2000.

[3] P. Srivaree-Ratana, "Lessons learned from the great Thailand flood 2011: How a UAV helped scientists with emergency response and disaster aversion," in *Proc. AUVSI Unmanned Syst. North Am.*, 2012.

[4] N. Michael, S. Shen, K. Mohta, Y. Mulgaonkar, V. Kumar, K. Nagatani, Y. Okada, S. Kiribayashi, K. Otake, K. Yoshida, K. Ohno, E. Takeuchi, and S. Tadokoro, "Collaborative mapping of an earthquake-damaged building via ground and aerial robots," *J. Field Robotics*, vol. 29, no. 5, pp. 832–841, 2012.

[5] S. Kawatsuma, M. Fukushima, and T. Okada, "Emergency response to Fukushima-Daiichi accident: summary and lessons learned," *Ind. Robot*, vol. 39, no. 5, pp. 428–435, 2012.

[6] R. R. Murphy, "Trial by fire," *IEEE Robotics Autom. Mag.*, vol. 11, no. 3, pp. 50–61, 2004.

[7] G.-J. Kruijff, V. Tretyakov, T. Linder, F. Pirri, M. Gianni, P. Papadakis, M. Pizzoli, A. Sinha, E. Pianese, S. Corrao, F. Priori, S. Febrini, and S. Angeletti, "Rescue robots at earthquake-hit Mirandola, Italy: A field report," in *Proc. IEEE Int. Symp. Saf. Secur. Rescue Robotics*, pp. 1–8, 2012.

[8] M. Arai, T. Takayama, and S. Hirose, "Development of Souryu-III: connected crawler vehicle for inspection inside narrow and winding spaces," in *Proc. IROS 2004*, 2004.

[9] A. Larson and R. Voyles, "TerminatorBot: A novel robot with dual-use mechanism for locomotion and manipulation," *IEEE/ASME Trans. Mechatronics*, vol. 10, no. 1, pp. 17–25, 2005.

[10] National Fire Protection Association, *Standard on Operations and Training for Technical Rescue Incidents*, Avon: NFPA, 1999.

[11] United States Fire Administration: Technical Rescue Program Development Manual (USFA, Avon 1996)

[12] A. Goriely, *The Mathematics and Mechanics of Biological Growth*, vol. 45. New York, NY: Springer, 2017.

[13] D. Weigel and G. Jürgens, "Stem cells that make stems," *Nature*, vol. 415, pp. 751–754, 2002. doi: 10.1038/415751a

[14] L. H. Blumenschein, N. S. Usevitch, B. Do, E. W. Hawkes, and A. M. Okamura, "Helical actuation on a soft inflated robot body," in *Proc. IEEE Int. Conf. Soft Robotics (RoboSoft)*, pp. 245–252, 2018. doi: 10.1109/ROBOSOFT.2018.8404927.

[15] E. W. Hawkes, L. H. Blumenschein, J. D. Greer, and A. M. Okamura, "A soft robot that navigates its environment through growth," *Science Robotics*, vol. 2, no. 8, 2017.

[16] M. M. Coad, L. H. Blumenschein, S. Cutler, J. A. R. Zepeda, N. D. Naclerio, H. El-Hussieny, et al., "Vine robots: design, teleoperation, and deployment for navigation and exploration," *IEEE Robot. Autom. Mag.*, vol. 27, pp. 120–132, 2020. doi: 10.1109/MRA.2019.2947538

[17] R. Niiyama, X. Sun, C. Sung, B. An, D. Rus, and S. Kim, "Pouch motors: printable soft actuators integrated with computational design," *Soft Robot.*, vol. 2, pp. 59–70, 2015. doi: 10.1089/soro.2014.0023

[18] J. D. Greer, T. K. Morimoto, A. M. Okamura, and E. W. Hawkes, "Series pneumatic artificial muscles (sPAMs) and application to a soft continuum robot," in *Proc. IEEE Int. Conf. Robotics and Automation (ICRA)*, Singapore, pp. 5503–5510, 2017. doi: 10.1109/ICRA.2017.7989648

[19] N. D. Naclerio and E. W. Hawkes, "Simple, low-hysteresis, foldable, fabric pneumatic artificial muscle," *IEEE Robotics Autom. Lett.*, vol. 5, no. 2, pp. 3406–3413, 2020.

[20] N. Naclerio, C. Hubicki, Y. Aydin, D. Goldman, and E. W. Hawkes, "Soft robotic burrowing device with tip-extension and granular fluidization," in *Proc. IEEE/RSJ Int. Conf. Intelligent Robots and Systems (IROS)*, Brisbane, QLD, pp. 5918–5923, 2018. doi: 10.1109/IROS.2018.8593530

[21] L. H. Blumenschein, M. M. Coad, D. A. Haggerty, A. M. Okamura, and E. W. Hawkes, "Design, modeling, control, and application of everting vine robots," *Frontiers in Robotics and AI*, pp. 153, 2020. doi: 10.3389/frobt.2020.548266

[22] C. Li, T. Zhang, and D. I. Goldman, "A terradynamics of legged locomotion on granular media," *Science*, vol. 339, pp. 1408–1412, 2013. doi: 10.1126/science.1229163

[23] L. H. Blumenschein, A. M. Okamura, and E. W. Hawkes, "Modeling of bioinspired apical extension in a soft robot," in *Biomimetic and Biohybrid Systems*, M. Mangan, M. Cutkosky, A. Mura, P. Verschure, T. Prescott, and N. Lepora, Eds., vol. 10384, *Lecture Notes in Computer Science*. Cham: Springer, 2017, pp. 446–457. doi: 10.1007/978-3-319-63537-8_45

[24] Z. Zhang, X. Wang, S. Wang, D. Meng, and B. Liang, "Shape detection and reconstruction of soft robotic arm based on fiber Bragg grating sensor array," in *Proc. IEEE Int. Conf. Robotics and Biomimetics (ROBIO)*, Kuala Lumpur, Malaysia, pp. 978–983, 2018. doi: 10.1109/ROBIO.2018.8665266